ELSEVIER

Microelectronics Journal 34 (2003) 115–126

Microelectronics Journal

www.elsevier.com/locate/mejo

Design and optimisation of a high-temperature silicon micro-hotplate for nanoporous palladium pellistors

S.M. Lee*, D.C. Dyer, J.W. Gardner

Smart Sensors and Devices Group, School of Engineering, University of Warwick, Coventry CV4 7AL, UK

Received 11 September 2002; revised 8 October 2002; accepted 15 October 2002

Abstract

The conventional design of the heater in a silicon micro-hotplate employ a simple meandering resistive track to form a square element. We show that this heater structure produces an uneven thermal profile characterised by a central hot spot with a significant variation in temperature of some 50 °C across the plate at an average temperature of 500 °C. Four novel micro-heater designs are reported here and fabricated on hotplates with an active area that ranges from (200 × 200) μm^2 to (570 × 570) μm^2 in order to vary systematically the ratio of membrane to heater length from a value of 5.0–2.7, respectively. All the designs have been simulated using a 3D electro-thermo-mechanical finite element model and results agree well with thermal profiles taken using an infrared microscope. One of the designs, referred to here as 'drive-wheel' structure, performs best and reduces the lateral variation in temperature to only ± 10 °C. The different resistive micro-heaters have been calibrated with the lowest power consumption being 50 mW at 500 °C, which is well below the power consumption of any commercial pellistor; the maximum temperature before rupture being 870 °C. The micro-hotplates were electrochemically coated with a 20 nm thick mesoporous palladium catalyst and the pellistors' response tested to 2.5% methane in air. The micro-heaters were observed to be stable for a period of 1000 h and should provide a good platform for exploitation in commercial catalytic pellistors.

Keywords: Silicon micro-hotplate; Pellistor; Catalytic gas sensor

1. Introduction

A pellistor is a type of micro-calorimetric sensor that is used to detect combustible gases, such as methane, in the atmosphere. Commercial pellistors comprise of a platinum coil encapsulated with alumina and coated with a layer of sintered porous palladium catalyst to form a small bead that is suspended between two metal pins inside a protective metal can, as shown in Fig. 1. A suitable voltage applied across the coil raises its temperature to about 500 °C. The high temperature causes the gas to combust and raises the temperature of the bead further. The resulting increase in electrical resistance of the platinum coil may be measured using a Wheatstone bridge circuit with a second inert pellistor acting as the balance arm. The output from a commercial pellistor is typically 50 mV for each percent of methane in air [1], at a high power consumption of 100–500 mW per element. The manufacturing process is very labour intensive and hence costly, so companies are looking towards silicon microtechnology to make micro-pellistors in high volume at lower unit cost with a power consumption that is compatible with battery-operated handheld gas monitors.

The concept of a silicon micro-pellistor was first published by Gall in the early 1990's, but early efforts did not lead to reproducible devices [2,3]. Since then silicon process technology has improved and a number of micro-hotplate designs have been reported for resistive gas sensors using either a membrane or suspended beam with a platinum or polysilicon resistive heater; these generally operate at a temperature of around 200 °C lower than that needed for a pellistor [4]. Here we have utilised a low-stress silicon nitride process developed at the Institute of Microtechnology (Neuchatel) for our micro-hotplate structures.

Furthermore, a novel, nanoporous palladium catalyst has been developed at Southampton University [5] and deposited upon our first design of a silicon micro-hotplate. Initial studies show that the device works well and has a level of resistance to the poison HMDS that exceeds any

* Corresponding author. Fax: +44-24-76-418-922.
E-mail address: esruh@eng.warwick.ac.uk (S.M. Lee).

0026-2692/03/$ - see front matter © 2002 Elsevier Science Ltd. All rights reserved.
PII: S0026-2692(02)00153-2

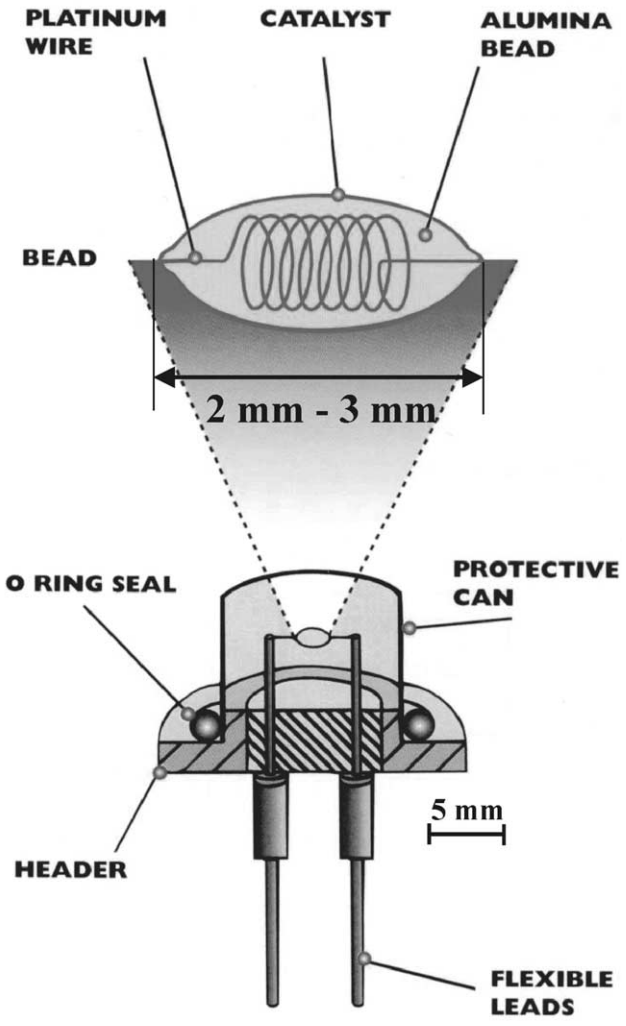

Fig. 1. Construction of a commercial pellistor [1].

current commercial products [6]. However, the power consumption of the micro hotplate was relatively high, i.e. similar to existing commercial products, had undesirable lateral temperature variation, and tended to fail at around 600 °C. Therefore, we have set out to design a new generation of silicon micro-hotplates that will provide a superior performance and hence be suitable for commercial applications.

2. Design and optimisation

The silicon micro-hotplate comprises of a thin platinum heater sandwiched between two silicon nitride layers and isolated from a ⟨100⟩ silicon 4 in. handle wafer, as shown in Fig. 2. The membrane consists of 50 nm thermal oxide, 250 nm low stress LPCVD silicon nitride, 250 nm of platinum, and then another 500 nm of silicon nitride making a total thickness of around 1000 nm. The electrical resistance of the platinum micro-heater was nominally set to 100 Ω, but in practice was varied according to the desired heater shape and size. Next, a 150 nm layer of gold was evaporated on top of the silicon nitride and patterned using a lift-off technique to form an electrode directly above the micro-heater that was subsequently used to electrodeposit the nanoporous catalyst. Finally, an additional 200 nm layer of silicon nitride was added to passivate the electrode tracks and so prevent the unwanted deposition of the catalyst on the gold track. The device was then back-etched in KOH both to define the membrane and to create snapping grooves to dice up the wafer.

The performance of the original micro-pellistor design (labelled here as SRL 136), as mentioned above, tended to suffer from an uneven thermal distribution across the heated area. This could, in turn, cause an uneven catalytic reaction and hence reduce the performance of the micro-pellistor. Although the gold electrode (and catalyst) help to spread out the thermal profile [7], Fig. 3 shows that a circular hot spot is clearly visible on the device. Although the power consumption is similar to that of a commercial pellistor, it is still too high for a hand-held battery-operated instrument. Moreover, the operating voltage of 8.5 V is higher than that currently found in commercial pellistors.

The original meandering heater design has now been optimised (SRL 162g) by reducing the size of the gold electrode to be exactly the same size as the underlying platinum micro-heater. Furthermore, the heater track coverage has been reduced from 70 to 55% in order to redistribute the heat to reduce the hot spot phenomenon.

Thermal loss from the micro-hotplate comes from three sources: conduction through the membrane, convection to air, and radiation. The convection loss depends principally upon the area of the heater and the radiation loss is negligible at the operating temperature [8]. The membrane should be thin and of a low thermal conductivity material to minimise the conductive heat loss [9]. The parameter that relates the side length of the membrane to heater size or membrane-to-heater ratio (MHR) is critical in setting both the power consumption and mechanical robustness of the device. The importance of this parameter has been reported elsewhere [10,11] and its poor setting can lead to a process yield of below 40% [12] and high power consumption. The MHR value is 3.5 for the new meandering design and this has resulted in a satisfactory process yield of over 90%. However, the basic meandering structure still produced a central hot spot and so three new designs were created with different die sizes as shown in Fig. 4 that we refer to as (a) the ultra-low resistance, (b) the honeycomb, and (c) the drive-wheel. It was believed that these structures would distribute the heat more uniformly over the heater area and so reduce the central hotspot described above. The parallel tracks are designed to reduce the overall resistance of the heater and so reduce the required operating voltage to below 5 V. For example, the circular drive-wheel design employs two resistive micro-heater tracks in parallel. The two platinum tracks form a circular pattern with the centre unheated.

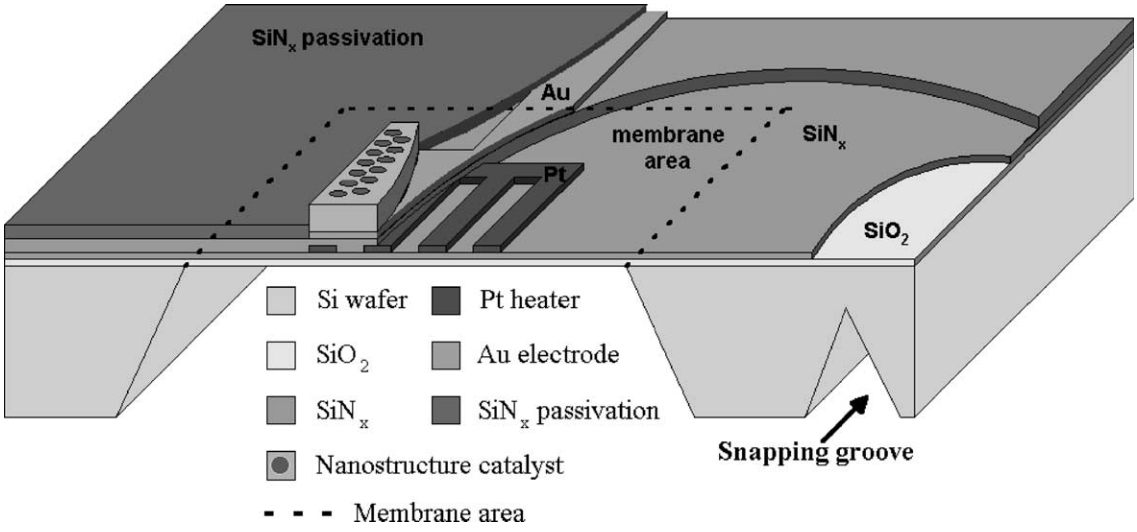

Fig. 2. Cross-section of the silicon planar micro-pellistor (not to scale).

Furthermore, the track separation is closer at the edge of the electrode and gradually increases towards the centre; the power input should be more evenly distributed and ideally eliminate the central hot spot. The track coverage had been increased to about 60% to improve the heating efficiency. The honeycomb design employs a strategy that redistributes the thermal energy by varying the width of the track. Therefore, its resistance is lowered to reduce the local power dissipated. The ideal micro-heater resistance was required to operate with a supply of 2.5 V and therefore designed to have a resistance of about 40 Ω. In addition, the value of the MHR was increased to 5:1 in order to reduce further the power consumption and increase the robustness of the device. Large and small versions of each design were developed to explore systematically the effect of heater size, membrane size, and MHR on the performance of the silicon micro-pellistor. The dimensions of the various designs are listed in Table 1.

3. 3D thermo-mechanical simulations

Full device simulations have been carried out in order to investigate the performance of the micro-hotplate

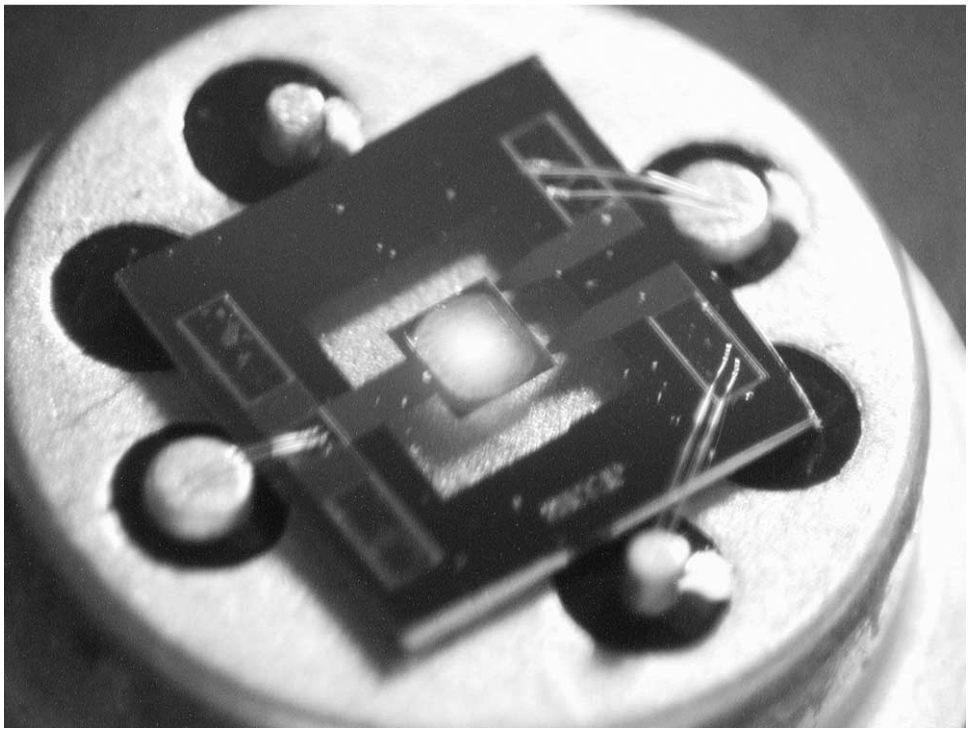

Fig. 3. Initial micro-hotplate design (SRL 136a). The active area glows at high temperature showing the circular thermal profile and local hot spot.

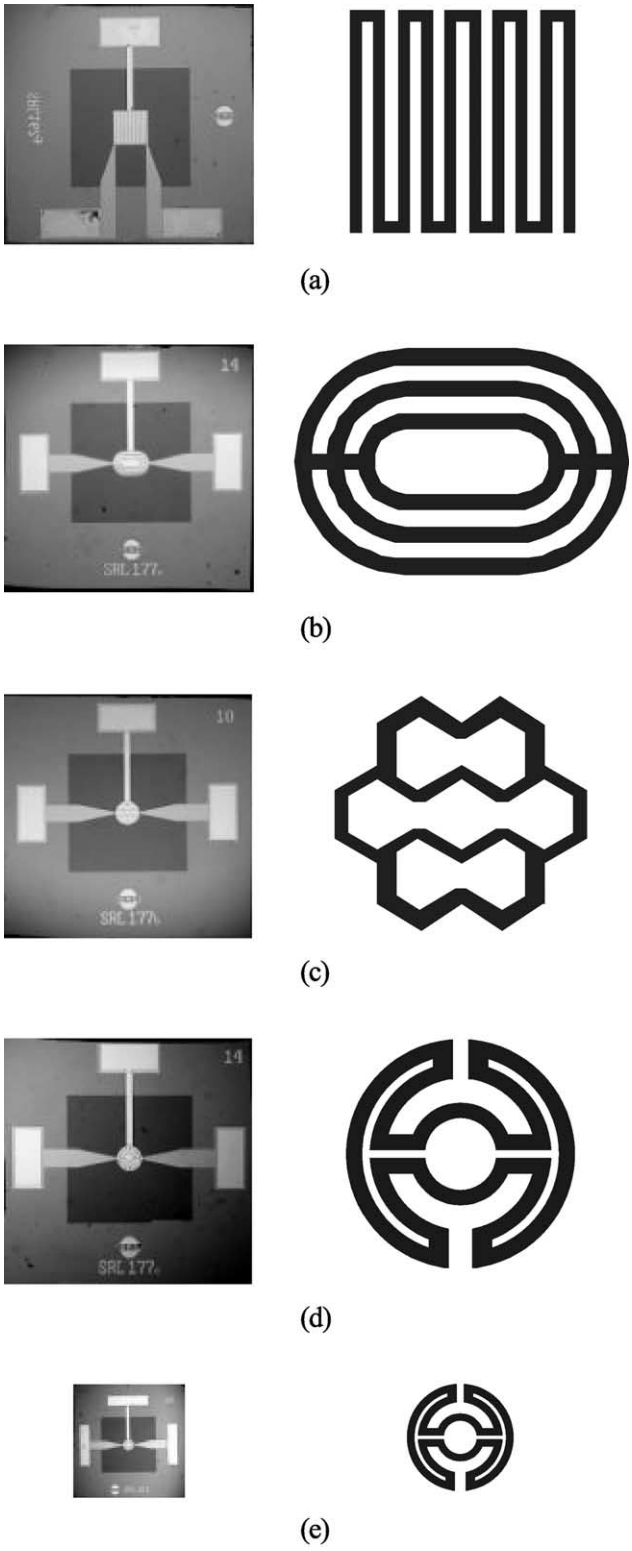

Fig. 4. The optimised micro-hotplate device with the schematic of the micro-heater designs. (a) The optimised meander design (SRL 162g); (b) the ultra-low resistance design (SRL 177a); (c) the honeycomb design (SRL 177b); (d) the drive-wheel design (177c) and (e) the ultra-miniature drive-wheel design (SRL 181c).

designs prior to the fabrication. A set of 3D simulations were conducted using SOLIDIS version 6.0 by Integrated System Engineering (ISE) that employs a finite element method (FEM) as the core of its simulation engine. Full 3D geometrical models were generated with exact dimensions of the micro-hotplates for all the designs. An example of the simulation model for each micro-heater design is shown in Fig. 5, whilst the geometries of the membrane and micro-heater have been modified to realise different MHRs. Note that the rectilinear meshing method of the simulation software prevents the creation of any curves for modelling. The simulation model of the new micro-heater design, such as the drive-wheel design, had to be approximated by straight edges, see Fig. 5(d).

In order to reduce the computational time, the model of the micro-hotplate excluded the silicon frame of the device and simulated only the membrane. Since the silicon nitride membrane provides remarkable thermal isolation, the temperature of the frame is assumed to remain at room temperature. Hence, the boundary condition was 300 K. A constant volumetric heat source of 6.525×10^{11} Wm^{-3} was applied and is equivalent to 100 mW input to the micro-heater with an expected average temperature of about 500 °C. The heat flux is set to flow from the constant heat source to the membrane while heat is dissipated into the air from both sides of the membrane by convection.

The precise values of the material properties required for the simulation software are not available because they vary from process to process. The effect of the layer thickness is probably small as the Sondheimer theory, which predicts that the material properties will not be altered significantly until the material thickness is less than 8% of its mean-free-path [13]. The values of the simulation parameters are given in Table 2 and are our best estimates.

Our simulation results for the optimised meandering design show that the central hot spot has been significantly reduced and it provides better thermal homogeneity, see Fig. 6(a). The circular thermal profile, location of the hot spot and its deflection agree with the physical observations. The simulation results in Fig. 6(b) shows a typical thermal profile of the drive-wheel design. It indicates that our new design has successfully eliminated the hot spot within the active area and the result has been confirmed by observing the fabricated devices with an infrared imaging system. The two other designs showed the presence of two smaller hotspots and so were abandoned in favour of the superior drive-wheel design. Finally, the 2D thermal profiles across the entire membrane for different micro-heater designs were compared against each other, as shown in Fig. 7. It clearly shows an improvement on the temperature uniformity within the active area.

Table 1
Various device types and their corresponding membrane size, heater size and MHR

Device code	Design type	Membrane size (mm × mm)	Heater size (μm^2)	MHR
SRL 136a	Former meander design	2 × 2	750 × 750	2.7
SRL 162g	Optimised meander design	2 × 2	570 × 570	3.5
SRL 177a	Ultra-low resistance design	2 × 2	400 × 600	3.3
SRL 177b	Honeycomb design	2 × 2	π $(200)^2$	5
SRL 177c	Standard drive-wheel design	2 × 2	π $(200)^2$	5
SRL 181c	Ultra-miniature drive-wheel design	1 × 1	π $(100)^2$	5

4. Fabrication details

4.1. Silicon micro-hotplate

The batch of wafers was processed at the Institute of Neuchatel (Switzerland) using a set of 5 masks made at Compugraphics Ltd (UK). The yield of each wafer (before dicing) was over 95% indicating that the MHR was optimised appropriately to provide sufficient mechanical strength. The devices were snapped out manually using the micro-machined snapping grooves and the yield of this step varied with experience. The devices were then mounted on a gold-plated TO5 package with a gap left at the back of the chip to allow for thermal expansion of the air under the membrane. Leads were connected by an ultrasonic wedge bonder with 25 μm diameter gold wire. The temperature coefficient of the platinum heater was determined experimentally and found to be linear with a resistance coefficient of $(1.66 \pm 0.05) \times 10^{-3}$/°C. The micro-hotplates were found to withstand a maximum temperature of 870 °C before rupture and had a power consumption ranging from 50 to 250 mW at a temperature of 500 °C. The values were consistent with both the results of our numerical simulations and previous work on silicon micro-machined resistive gas sensors [8].

4.2. Catalyst deposition

A nanostructured catalyst was deposited on to the micro-hotplate using a novel approach recently invented by Southampton University [14]. A lyotropic mixture was prepared based on an aqueous C16E08.3 system that self-assembles into a hexagonal close-packed nanostructure (Fig. 8(a)) when applied to the surface of the device. Then the catalyst (i.e. palladium) was grown electrochemically around the lyotropic film on top of the gold electrode that

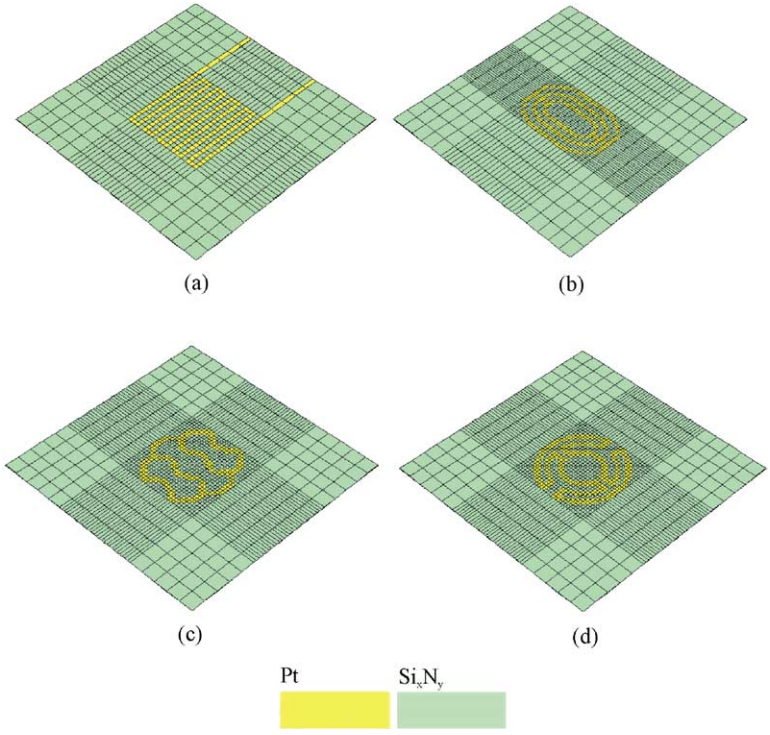

Fig. 5. 3D micro-heater geometrical models for electro-thermo-mechanical simulation. The Au gate electrode and the encapsulating silicon nitride are not shown so as to reveal the micro-heater. (a) The optimised meander design (SRL 162g); (b) the ultra-low resistance design (SRL 177a); (c) the honeycomb design (SRL 177b); (d) the drive-wheel design (SRL 177c).

Table 2
Material properties employed in the electro-thermo-mechanical FEM simulations. The values shown here are at 300 K while the model accounts for different operating temperatures

Property	Units	Pt	Au	Si_xN_y	SiO_2	Si
Thermal conductivity (κ)	W/m K	73	315	22	1.4	157
Elasticity modulus (Young's modulus)	GPa	170	80	290	73	190
Poisson's ratio	–	0.39	0.42	0.24	0.20	0.17
Thermal expansion (β)	1/K	8.9×10^{-6}	14.3×10^{-6}	2.33×10^{-6}	0.55×10^{-6}	2.33×10^{-6}
Density (ρ)	kg/m^3	2.145×10^4	1.932×10^4	3.1×10^3	2.2×10^3	2.32×10^3
Heat capacity (C_p)	J/kg °C	130	130	600–800	730	700

forms the working electrode. Finally, the lyotropic film was washed away in water to leave a nanoporous layer of catalyst (Fig. 8(b)). This templating method produces a uniform catalytic film with a very high surface area (about 20 m^2/g) because the nanopores are only about 2.5 nm in diameter and separated by walls of 2.5 nm thickness. The precise structure and composition of the catalytic film can be controlled by the deposition conditions and electrochemical process. The thickness of the catalytic layer is controlled by the deposition time and the charge density supply to the gold working electrode. This deposition process can be extended from single device deposition to wafer-level deposition and the skill required is reduced significantly in contrast with classical pellistor production. See Ref. [6] for further details.

5. Thermal characterisation

5.1. Electrical

A batch of silicon micro-machined devices were characterised in order to determine their general performance. The temperature dependence of the micro-hotplate is determined by the temperature coefficient of resistivity (α) of the platinum resistor and its resistance at ambient temperature (R_0). These two parameters were calculated by measuring the resistance of the platinum micro-heater R_T at different temperatures T and using the following linear equation:

$$R_T = R_0(1 + \alpha(T - T_0)) \quad (1)$$

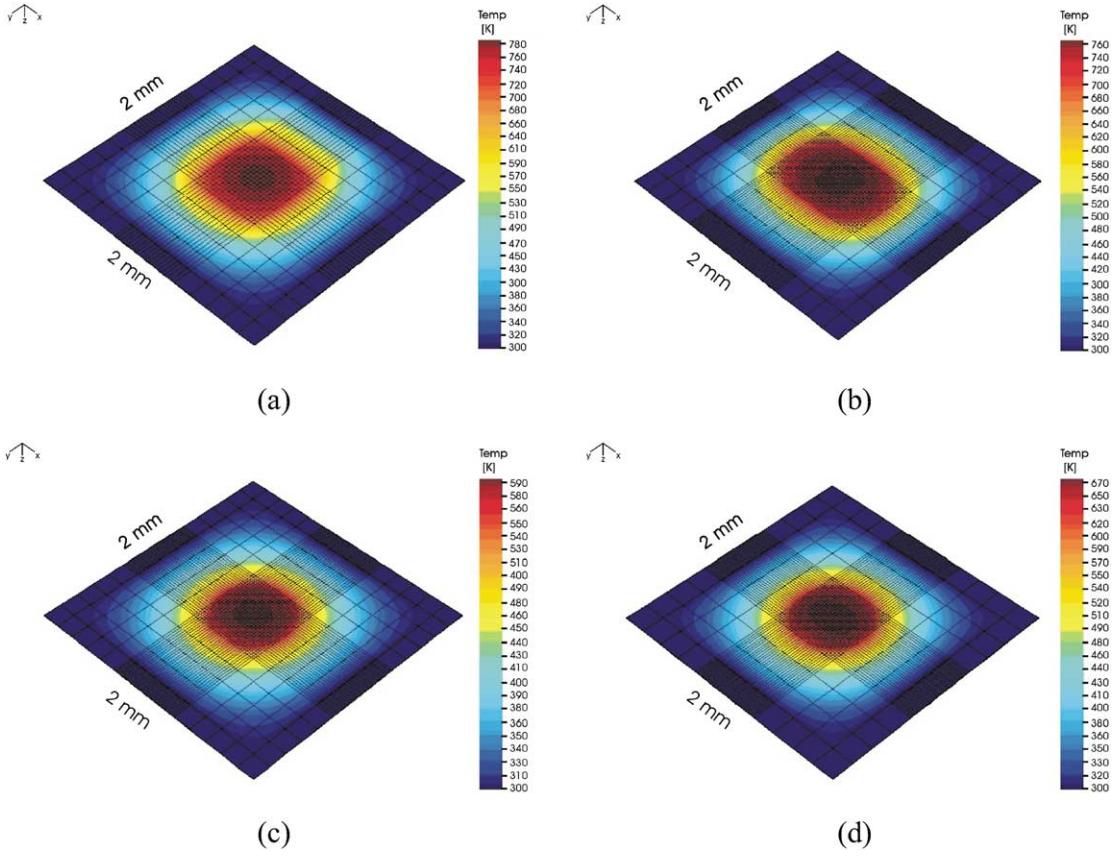

Fig. 6. 3D electro-thermo-mechanical simulation results with an input power of 100 mW. (a) The optimised meander design (SRL 162g); (b) the ultra-low resistance design (SRL 177a); (c) the honeycomb design (SRL 177b); (d) the drive-wheel design (SRL 177c).

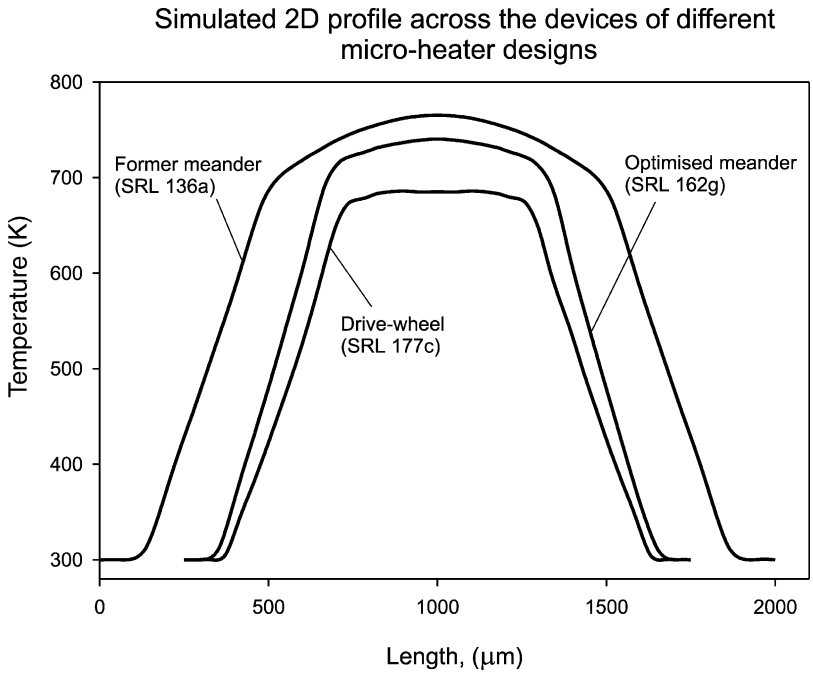

Fig. 7. The 2D profiles of the active area for various designs, indicating the improvements with optimised micro-heater designs.

Measurements were made from room temperature to 600 °C to obtain the near linear plots shown in Fig. 9. Not only do they provide the base-line resistance (R_0) and the temperature coefficient of resistance (α), but also allow us to find the temperature of the active area during operation. To be precise, the temperature computed actually represents the average temperature of a resistive track micro-heater with a constant width and hence provides a good estimate of the average temperature of the active area for the micro-hotplate.

The power consumption (I^2R_T) of the device was then calculated based on the measurements from a constant current (I) circuit. The data were compiled and analysed for the device performance, using a mathematical model of the total power loss, Eq. (2a). This equation consists of three terms, namely, conduction loss via the membrane, P_c, convective loss to air, P_v, and radiative loss, P_r.

$$P = P_c + P_v + P_r \tag{2a}$$

The corresponding heat loss terms can be related to temperature as shown in Eq. (2b) [7], where P is the power, T is the micro-heater temperature and T_0 is the ambient temperature. The model was used to estimate the power consumption against the temperature generated by the heater. The results are shown in Fig. 10.

$$P = a(T - T_0) + b(T - T_0)^2 + c(T^4 - T_0^4) \tag{2b}$$

where a, b, c are physical constants

The results proved that the power consumption of the new design was significantly lower that that of the original design. For example, there is a 60% saving in the ultra-miniature design at 500 °C. Therefore, increasing the MHR is a sensible strategy for minimising the power budget. A MHR optimisation model has been derived empirically, relating the length of the device and the MHR. This is of assistance in the further development of similar devices, as shown below

$$P_e = l(65.6 - 22.5 \ln[\mathrm{MHR}]) \tag{3}$$

where the length l of the device is in units of mm and the estimated power (P_e) is in milliwatts.

The requirement to reduce the micro-pellistor drive voltage has been achieved with the meander design, SRL 162g, having a value of 6.5 V and the drive-wheel designs, SRL 177c and SRL 181c, from 2 to 3 V. Hence, the micro-pellistors with the drive-wheel design are compatible with battery-operated interface circuitry.

The result also indicates that the meander type micro-heater provides an optimal heating efficiency with an inevitable local hot spot. The drive-wheel micro-heater design achieved an isothermal active area but the heating efficiency has been reduced simultaneously.

Comparing the same cell size and micro-heater design, the power reductions for the devices are inversely proportional to the MHR parameter. Although the MHR of the ultra-miniature and the standard drive-wheel designs are identical, their overall geometry is different. The ultra-miniature design reduces the surface area for convectional heat loss and leads to lower power consumption.

Therefore, power optimisation of a device will depend on the MHR, overall geometry and the micro-heater design. Compromises will have to be made when customising a device to satisfy the power requirement for specific applications.

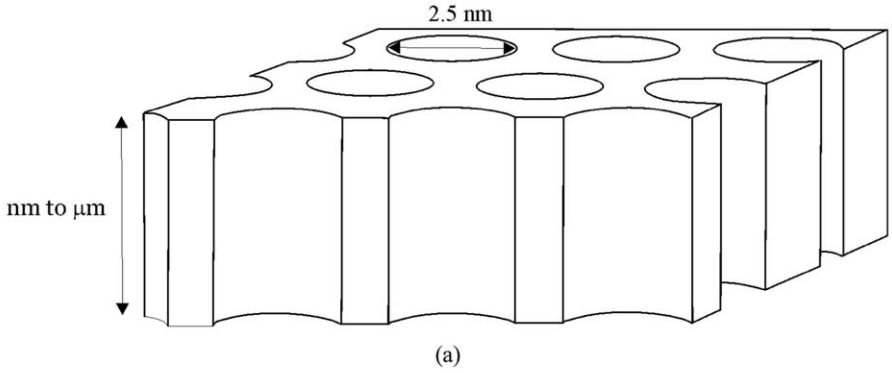

(a)

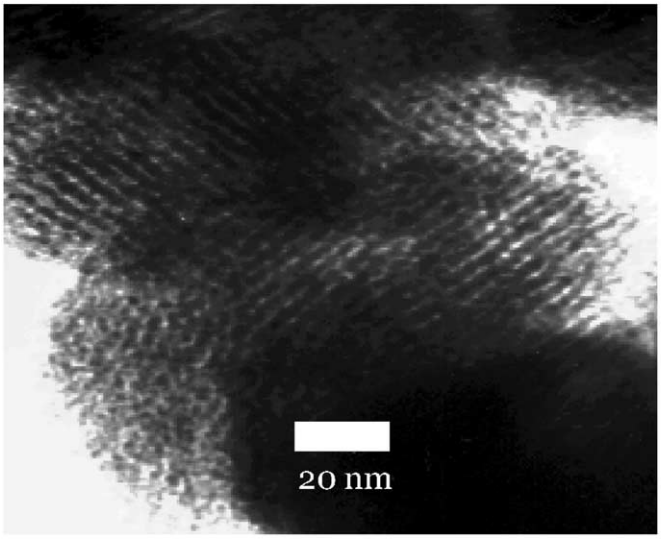

(b)

Fig. 8. The nanoporous palladium catalyst. (a) 'Cartoon' of the self-assembled nanostructured catalyst film (not to scale); (b) transmission electron micrograph of the nanoporous Pd film showing the hexagonal close-packed structure.

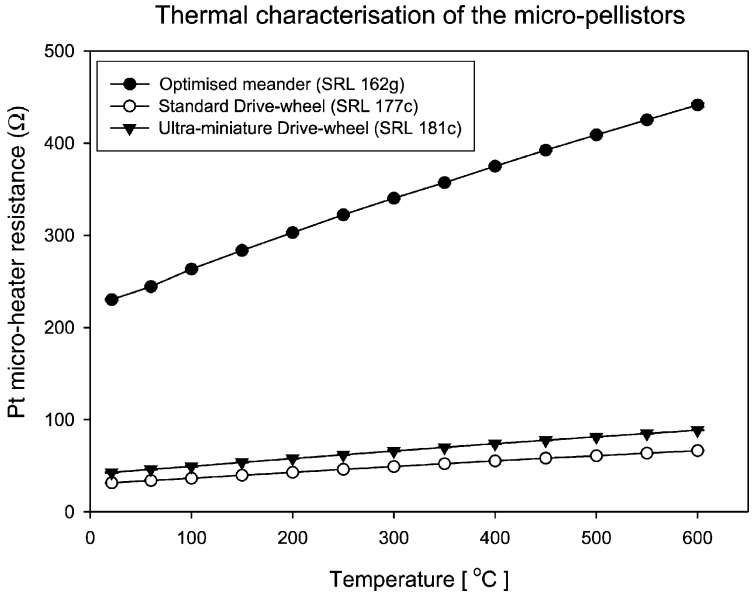

Fig. 9. Thermal characterisation results of the micro-pellistors employ different micro-heater designs, error bars included but not visible due to negligible tolerances.

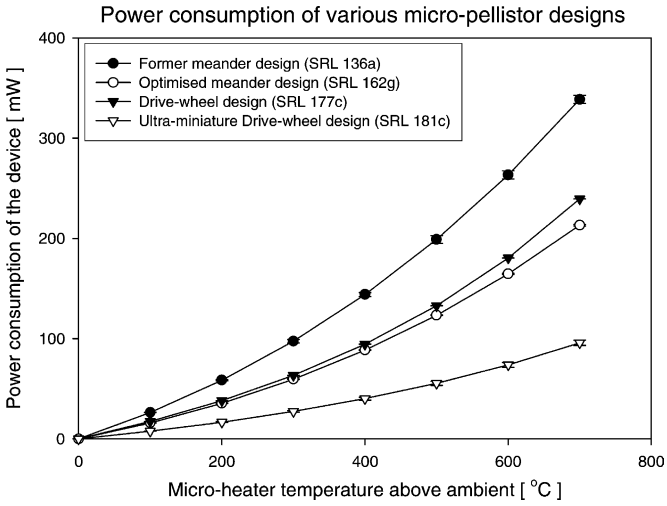

Fig. 10. Power consumption of the various micro-pellistor designs.

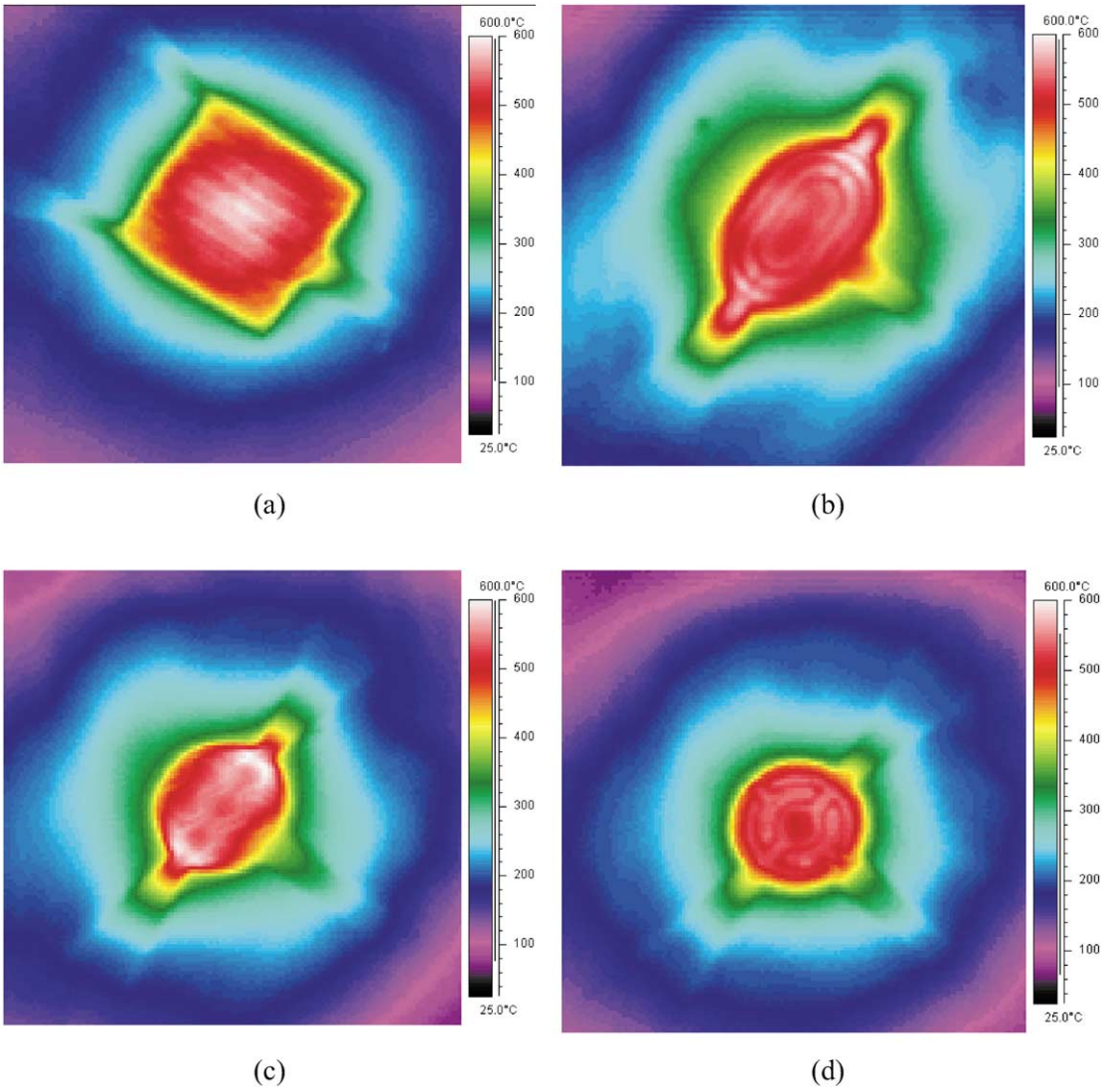

Fig. 11. Thermal images of the active area. (a) The optimised meander design (SRL 162g) showing the hot spot at the centre; (b) the ultra-low resistance design (SRL 177a) showing two hot spots at both ends of the micro-heater; (c) the honeycomb design (SRL 177b), showing two hot spots again; (d) the drive-wheel design (SRL 177c) with remarkable temperature homogeneity.

5.2. Infrared imaging

The active area thermal distribution of the devices has been investigated using an infrared microscope, as shown in Fig. 11, with a thermal accuracy of ± 2 °C. It comprised an Agema Thermovision 880 infrared camera attached to a microscope with a controlling computer, TIC-8000. For the meander type micro-heater design, a central hot spot was observed and the thermal profile is indeed circular as predicted by the simulation results. The thermal profile for the ultra-low resistance and the honeycomb design showed two smaller hot spots that were not predicted in the simulation, see Figs. 11(b) and (c). Fig. 11(d) indicated that the drive-wheel micro-heater design has successfully reduced the hot spot and created a larger isothermal active area. The standard deviation of the temperature, up to 10 °C, across the gold electrode has been achieved for the drive-wheel design operating at 500 °C. This is an acceptable temperature variation for the known temperature sensitivity of the catalyst's response and we believe to be the lowest value achieved to date.

6. Micro-pellistor performance

6.1. Response to methane (CH_4)

A layer of nanostructured catalyst was deposited onto the micro-hotplate with a thickness of about 100 nm with specific surface area of about 8 m^2/g. A batch of nanoporous palladium silicon micro-pellistors were tested employing a Wheatstone bridge system and an automated gas testing station, which is currently used for commercial pellistors at City Technology Ltd. Fig. 12 shows the response of the different micro-pellistor designs with the methane concentration set at 50% of the lower explosive limit, i.e. 2.5% in air and a flow rate of 300 ml/min. The Wheatstone bridge output indicated that the optimised meander design has given the highest voltage output. However, maximum output magnitude does not necessarily reflect the catalyst's reaction because the output magnitude also depends upon the initial bridge voltage.

The reactivity of the catalyst can best be defined as the temperature increase per percent methane in air. As the area of the electrode for the various designs is different (see Table 1), the catalyst's reactivity should be normalised against the volume of catalyst, as shown in Fig. 13(a). The ultra-miniature and the optimised design, employing the drive-wheel micro-heater design, show high reactivity due to the larger isothermal active area. The more uniformly heated electrode permits a greater amount of the catalyst to reach its ideal operating temperature and hence a higher output voltage.

It is important to note that the temperature increase due to the catalyst's reaction also depends on the thermal mass of the membrane. Thus, the MHR is an important parameter to be considered when optimising the catalyst's reaction.

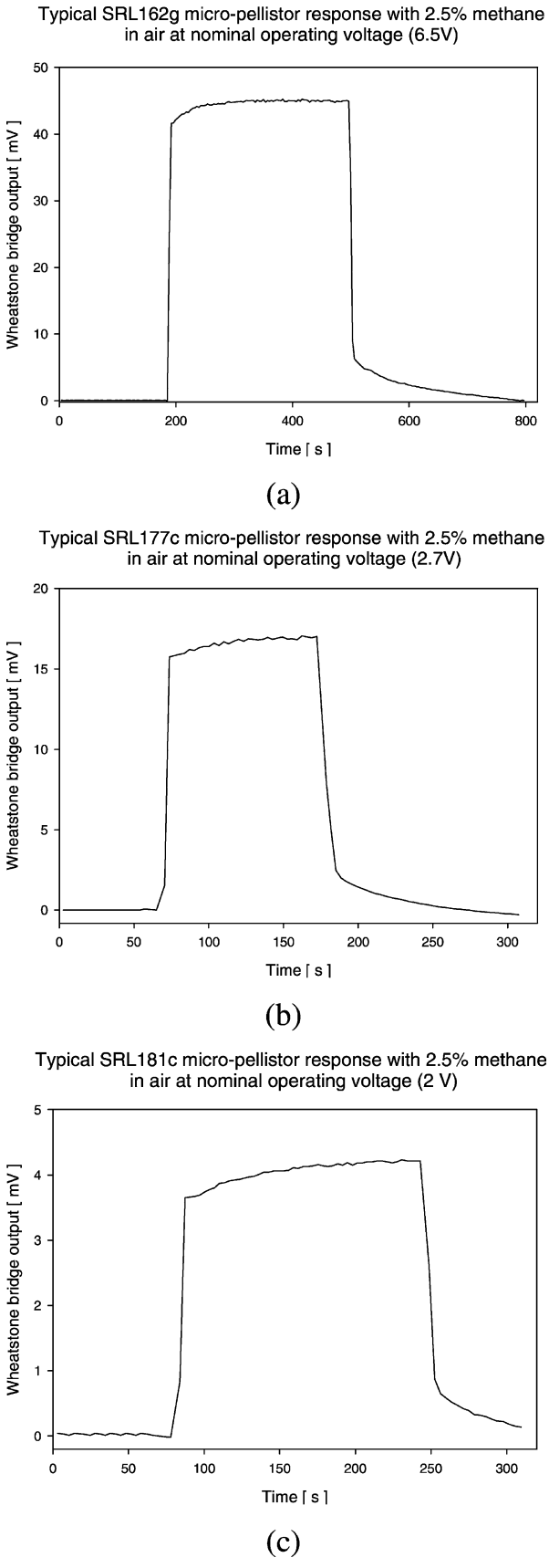

Fig. 12. The device responses for 2.5% methane in air. (a) Optimised meander design; (b) drive-wheel design; (c) ultra-miniature drive-wheel design.

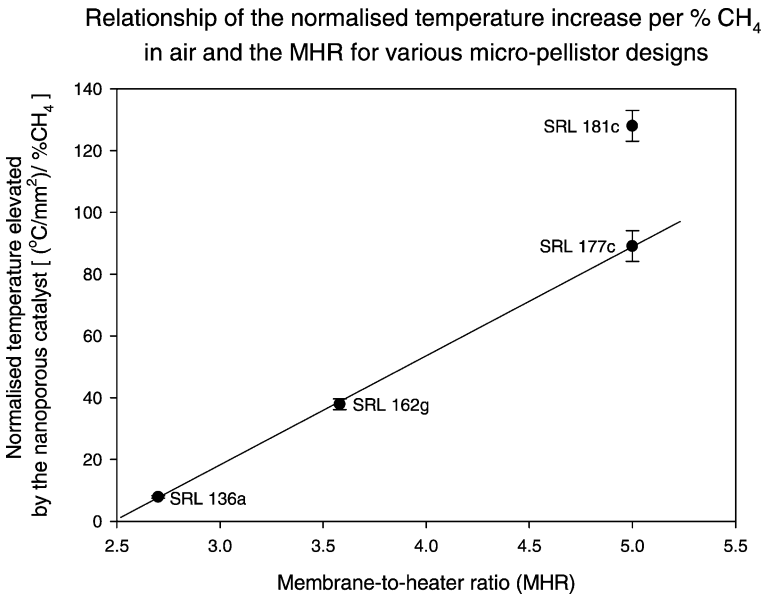

(a)

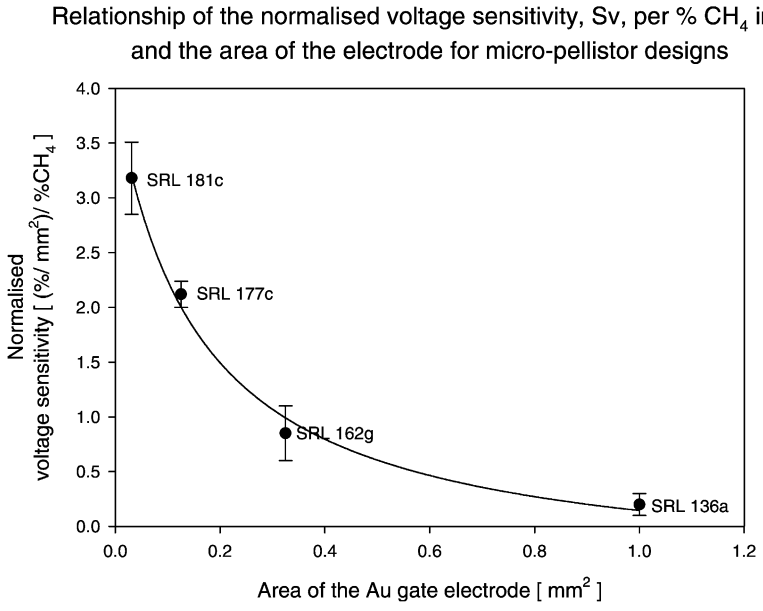

(b)

Fig. 13. Analysis of the catalyst's efficiency. (a) The normalised temperature increase indicated that the optimised devices improved the catalyst's reactivity with a linear relationship for identical chip size; (b) the catalyst's efficiency for the optimised devices is higher, in spite of smaller amount of catalyst. An inversed second order polynomial fitting indicated that the sensitivity is inversely proportional to the area of the electrode.

Fig. 13(a) shows the relationship between the normalised temperature increase per percent of methane in air and the MHR of the devices. It proves that higher the MHR, higher the temperature increase by the catalyst. When the influence of the MHR has become saturated, the overall geometry of the device will continue to affect the temperature output. Therefore, although the ultra-miniature and the optimised design have identical MHRs, the temperature increase is higher than for the other design.

The Wheatstone bridge sensitivity, S_v, is defined in Eq. (4), where V_{out} is the differential bridge output, V_{in} is the supply voltage and C is the gas concentration.

$$S_v = \frac{dV_{out}/V_{in}}{dC} \times 100\% \quad (4)$$

Fig. 13(b) shows the normalised bridge sensitivity against the area of the gold electrode. Apart from the supply voltage, the output magnitude depends on the area of catalyst available for reaction. Although the electrode area of the former design is the largest, all the optimised designs achieved higher sensitivity for methane detection. Furthermore, despite having the minimum quantity of catalyst, the ultra-miniature

design achieved the highest sensitivity. Therefore, it can be seen that the optimisation of the initial design has improved the performance of the micro-pellistor. However, it has also been shown that the maximum catalytic reactivity does not necessarily produce the maximum bridge output. It also implies that the optimisation should be performed cautiously in order to achieve the require performance.

6.2. Long-term reliability and transient behaviour

The stability of the silicon micro-hotplate device was investigated in an experiment that involved the continuous powering of the heater for a period of 1000 h with a constant current provided by a Knick DC Calibrator unit. There was negligible change in the resistance of the device under these test conditions. Next, the test was made more stringent by powering the micro-heater cyclically with a frequency of 1 Hz for another 1000 h. Again, the device showed no significant change in characteristics. It should be noted that the top passivation layer of silicon nitride was found to improve the mechanical robustness of the membrane and permit slightly higher operating temperatures (870 °C before rupture) and is recommended for future use. The balancing micro-pellistor was found, as expected, to remove common mode variations such as a change in ambient temperature. The configuration should also remove the affect of any ageing of the micro-heater, one possible mechanism being the diffusion of the gold electrode into the nitride membrane and eventual reduction in heater resistance. The nitride is 500 nm thick and for a diffusion coefficient of gold into silicon nitride of 1.0×10^{-18} cm^2/s, this would take approximately 20 years.

Finally, the rise (and fall) time of the silicon micro-pellistor (SRL 177c) and a commercial pellistor (P50, City Technology Ltd) were measured in a preliminary study using a function generator (Philips PM5168) with a buffer circuit to boost the current drive and a digital storage scope (Tektronics TDS 210). The time taken to reach 500 °C from ambient was found to be about 4 ms (t_{90} value) and it is about 25 times quicker than the commercial pellistor which took about 100 ms. This ultra-fast time-constant offers the possibility of additional power savings by operating the device in a pulsed mode. We estimate that the power consumption could be reduced by a factor of at least 5 and still satisfy UK safety legislation [15]. Experiments that are more detailed are underway with gas testing and will be reported elsewhere.

7. Conclusions

We have created some new designs of silicon micro-hotplates for use in nanoporous micro-pellistors. The new designs have led to a device with a 60% reduction in its power consumption at 500 °C. Moreover, a novel drive-wheel micro-heater has been shown to produce not only a more uniform temperature profile but also to yield a higher catalytic efficiency. The transient thermal response of the optimised devices has been shown to be at least 25 times faster than existing commercial pellistors and to offer the potential for further power savings. The device had also been operated continuously for a period of 1000 h at 500 °C followed by thermal cycling at 1 Hz for further 1000 h without failure. When the outstanding poison-resistance of the nanoporous catalyst, reported previously, is considered this device shows significant potential for commercial exploitation.

Acknowledgements

The authors thank Dr M. Willett and Dr S. LeClerc at City Technology Ltd, UK, for their financial support of this project and Prof. P.N. Bartlett and Mr J. Marwin at Southampton University for the deposition of the nanoporous catalyst. They also thank Dr D. Briand and Prof. de Rooij at the Institute of Microtechnology (Neuchatel) for processing the wafers.

References

[1] Product data handbook, 4-Series PDH for portable safety application (issue 2.2), City Technology Ltd, 1999, p. 44.
[2] M. Gall, The Si planar pellistor array, a detection unit for combustible gases, Sensors Actuators B 15/16 (1993) 260–264.
[3] M. Gall, The Si planar pellistor: a low-power pellistor sensor in Si thin-film technology, Sensors Actuators B 4 (1991) 533–538.
[4] Z. Tang, S.K.-H. Fung, D.T.-W. Wong, P.C.-H. Chan, J.K.-O. Sin, P.W. Cheung, An integrated gas sensor based on thin oxide thin-film and improved micro-hotplate, Sensors Actuators B 46 (1998) 174–179.
[5] G.S. Attard, J.C. Glycle, C.G. Göliner Liquid-crystalline phases as templates for the synthesis of mesoporous silica, Nature 378 (1995) 366.
[6] P.N. Bartlett, S. Guerin, J. Marwan, J.W. Gardner, S.M. Lee, M.J. Willett, S.A.A. Leclerc, A micromachined planar pellistor using an electrochemically deposited nanostructured catalyst, proceedings for the Symposium on Microfabricated Systems and MEMs V. Spring meeting of the Electrochemicals society, Philadelphia, USA, 17-22 May 2002 pp 24–31.
[7] J.W. Gardner, S.M. Lee, P.N. Bartlett, S. Guerin, D. Briand, N.F. de Rooij, Silicon planar microcalorimeter employing nanostructured films, Digest of technical papers, vol 1, Transducers'01 Eurosensors XV, 2001, p. 820–3.
[8] A.C. Pike, J.W. Gardner, Thermal modelling of micropower chemoresistive silicon sensors, Sensors Actuators B 45 (1997) 19–26.
[9] S.B. Crary, Thermal management of integrated microsensors, Sensors Actuators 12 (1987) 303–312.
[10] U. Dibbern, A substrate for thin-film gas sensors in microelectronic technology, Sensors Actuators B 2 (1990) 63–70.
[11] T. Neda, K. Nakamura, T. Takumi, A polysilicon flow sensor for gas flow meter, Sensors Actuators A 54 (1996) 626–631.
[12] S. Astie, A. Mgue, E. Scheid, L. Lescouzeres, A. Cassagnes, Optimisation of an integrated SnO_2 gas sensor using a FEM simulator, Sensors Actuators A 69 (1998) 205–211.
[13] K.L. Chopra, Thin Film Phenomena, McGraw-Hill, New York, 1969.
[14] G.S. Attard, P.N. Barrlett, N.R.B Coleman, J.M. Elliott, J.R. Owen, J.H. Wang, Mesoporous platinum films from lyotropic liquid crystalline phases, Science 278 (1997) 838–840.
[15] British Standard Institute, Instrument for the detection of combustible gases, British Standard BS 6020, 1982.